

# HIGH-RESOLUTION B-SCAN BEARING ESTIMATION USING THE FAST ORTHOGONAL SEARCH

Donald R. McGaughey<sup>1</sup>, Filip Bohac<sup>2</sup>, and Richard F Marsden<sup>1</sup>

<sup>1</sup> -Royal Military College of Canada, P.O. Box 17000, Station Forces, Kingston, Ontario

<sup>2</sup> - Acoustic Data Analysis Centre (Atlantic), P.O. Box 99000, Station Forces, Halifax, Nova Scotia

## ABSTRACT

A directional DIFAR passive sonobuoy has an omni-directional channel and two orthogonal directional channels. Acoustic targets can be detected on a plot of the power-spectral density of the omni-directional channel called a LOFARGRAM. In addition, a bearing estimate can be formed by the arctangent of the sine channel over the cosine channel (B-scan estimate). Traditionally, the fast-Fourier transform has been used to perform the estimate of the power-spectral density. The fast orthogonal search (FOS) algorithm has been shown give a higher resolution spectral estimate than the FFT algorithm. The power-spectral estimate of the FOS algorithm has been used instead of the FFT in generating the LOFARGRAM and B-scan bearing estimates. It is shown in simulation and experimental data that using the FOS algorithm allows two targets, whose frequencies are spaced closer than the FFT resolution, to be resolved. By resolving two targets, two bearing estimates are calculated and the resulting estimates are much more accurate than the FFT based B-scan bearing estimates.

## SOMMAIRE

Un DIFAR directionnel à bouée sonar passive a un canal omnidirectionnel et deux canaux à directions orthogonales. Les cibles acoustiques peuvent être détectées à partir d'une représentation graphique de la densité spectrale de puissance du canal omnidirectionnel, appelée LOFOGRAM. En outre une estimation du roulement peut être obtenue à partir de l'arctangente du canal sinus divisé par le canal cosinus (estimation de type B-scan). L'algorithme de Fast Fourier Transform est traditionnellement utilisé pour parvenir à une estimation de la densité spectrale de puissance. L'algorithme de Fast Orthogonal Search (FOS) produit une estimation de plus haute résolution spectrale que l'algorithme de FFT. L'estimation de la densité spectrale de puissance obtenue par l'algorithme de FOS a été utilisée à la place de la FFT pour la génération du LOFARGRAM et pour les estimations par B-scan de roulement. Il est démontré à partir de simulations et de données expérimentales que l'utilisation de l'algorithme FOS permet la détermination de deux cibles dont les fréquences sont plus proches que la résolution de la FFT. À partir de la détermination de deux cibles, deux estimations du roulement sont calculées de manière beaucoup plus précise que par l'estimation du roulement par B-scan basé sur la FFT.

## 1. INTRODUCTION

A directional frequency analysis and recording (DIFAR) sonobuoy is a passive acoustic sensor with three co-located hydrophones. The omni-directional sensor measures the overall acoustic pressure, while the sine and cosine sensors are orthogonal directional sensors [1]. Many Navies use the expendable DIFAR sonobuoy to detect and estimate the bearing of potential targets.

Traditionally, a power spectral density (PSD) of the omni channel is used to detect the presence of a target. The PSD is calculated over a short time-period and the PSD is plotted as a single line on a graph with the intensity of the PSD scaled as brightness. Each new PSD slice is placed at the bottom of the image – displacing all other slices upwards. The general term for a frequency versus time plot is a low-frequency analysis and recording spectrogram (abbreviated as LOFARGRAM),

or simply a gram [1].

The incident direction of an incoming acoustic signal can be computed using the arctangent of the cross-correlations of the sine channel over the cosine channel. A display of bearing versus frequency is known as a B-scan display [2]. Targets can be localized by operator identification of frequencies of interest and finding the corresponding bearing from the B-scan display.

These techniques require a trained operator to analyze the results. Although newer algorithms, such as the maximum likelihood adaptive beamforming (MLAB) [3], exist, the LOFARGRAM and B-scan algorithm are still used extensively. Thus in this paper, we present a simple modification to the LOFARGRAM and B-scan algorithms that improves the ability to detect and estimate the bearing of two targets that are narrowly separated in frequency.

The arctangent bearing calculation technique introduces errors when two sources in the same frequency bin lie at different bearings [3, 4]. In the case of sources of similar amplitudes, the single bearing will lie between the actual bearings of the two sources. If the two sources are of unequal amplitudes, the calculated bearing will lie closer to the stronger source, an effect known as bearing bias.

The PSDs required for the LOFARGRAM and B-scan are typically calculated using the fast Fourier transform (FFT) algorithm. It is well known that the frequency resolution of the FFT is inversely proportional to the record length of the time series [5, 6]. Thus, if two narrowband sources are in the same frequency bin, they will not be able to be separated in the LOFARGRAM and the B-scan will exhibit bearing bias as discussed above.

For a sampling frequency of  $f_s$  and a record length of  $N$  samples, the FFT resolution is known to be  $f_s/N$  [5, 6]. The fast orthogonal search (FOS) algorithm has been shown to give a PSD estimate with up to 10 times the resolution of the FFT [7-11]. Note that the FOS frequency resolution is dependent upon the signal and noise present in the record being modelled. Thus targets which may be in the same bin in the FFT spectral estimate may be resolved by the FOS spectral estimate.

In this paper the FOS spectral estimate has been used instead of the FFT spectral estimator in the LOFARGRAM and B-scan algorithms. The increased frequency resolution allows the resolution of two targets that are in the same FFT bin but not the same FOS bin. In addition, in this scenario, two unbiased directional estimates can be found by the B-scan algorithm.

In Section 2 the LOFARGRAM and B-scan algorithms are given in detail. In Section 3 a brief overview of the FOS algorithm for use in spectral estimation is provided. In Section 4, the modified B-scan and LOFARGRAM that use FOS for the spectral estimate are explained. Section 5 provides a comparison of the FOS-based and FFT-based algorithms on simulated data, while Section 6 compares the algorithms on real data from a sonobuoy. Section 7 provides results and conclusions.

## 2. LOFARGRAM AND B-SCAN ALGORITHMS

The output of the DIFAR sonobuoy is three separate time series: one for each the omni, sine and cosine channels respectively. The three time series are related by:

$$\begin{aligned} x_{ok} & \text{ Omnidirectional Channel} \\ x_{sk} &= x_{ok} \sin \theta \quad \text{Sine (East-West) Channel} \\ x_{ck} &= x_{ok} \cos \theta \quad \text{Cosine (North-South) Channel} \end{aligned} \quad (1)$$

where  $x_o$ ,  $x_s$ , and  $x_c$  are the omni, sine and cosine channels respectively and  $k$  is the sample number.

Targets of interest are located by plotting the power spectral density (PSD) of the omni channel and locating the frequencies which contain the highest energies.

For a sampled time series, the discrete Fourier transform (DFT) can be computed using [5]

$$X(k) = \frac{1}{N} \sum_{n=0}^{N-1} x(n) e^{-2\pi jkn/N} \quad (2)$$

In general, the power spectral density (PSD) is obtained from [5]

$$\Phi(k) = X(k)X(k)^* = |X(k)|^2 \quad (3)$$

where  $X(k)$  is the Fourier transform of the time series  $x(n)$ , and  $*$  indicates a complex conjugate.

The frequency resolution is defined as the minimum separation between two sinusoidal frequencies such that both frequencies can still be identified. For the DFT, the frequency resolution can be shown to be [5]

$$f_{res} = \frac{f_s}{N} = \frac{1}{NT_{sample}} = \frac{1}{T_{record}} \quad (4)$$

where  $f_s$  is the sampling frequency,  $N$  is the number of samples in the time series, and  $T_{sample}$  and  $T_{record}$  are the sampling and record period respectively. For example, a desired resolution of 0.25 Hz requires a sampling time of 4 seconds.

The LOFARGRAM requires the PSD of the omni channel which is given by

$$\hat{\Phi}_{oo} = \langle X_o X_o^* \rangle = \langle |X_o|^2 \rangle \quad (5)$$

where the angle brackets denote ensemble averaging, and the caret (^) indicates an estimated value. The frequency index  $k$  has been dropped for convenience.

Likewise, a PSD is computed for the cross-spectra between the channels

$$\begin{aligned} \hat{\Phi}_{os} &= \langle X_o X_s^* \rangle = \langle X_o X_o^* \sin \theta \rangle \\ \hat{\Phi}_{oc} &= \langle X_o X_c^* \rangle = \langle X_o X_o^* \cos \theta \rangle \end{aligned} \quad (6)$$

where  $\hat{\Phi}_{os}$  and  $\hat{\Phi}_{oc}$  are the *omni-sine* and *omni-cosine* cross-spectra, respectively.

Since a single time-series is being processed, a time-average of non-overlapping segments is used instead of an ensemble average. It is known that the variance of the PSD estimate from one segment is proportional to the magnitude of the PSD [5]. To reduce this uncertainty, typically the PSD from  $M$  non-overlapping time sequences are averaged, reducing the variance of the estimate by  $1/M$ . Windowing was not used in the PSD estimates of the FFT based LOFARGRAM.

The cross spectra are used to calculate the direction of arrival to a target of interest (TOI). The quotient of the omni-sine and omni-cosine PSD estimates yields a bearing from the simple trigonometric identity

$$\hat{\theta} = \arctan \left( \frac{\hat{\Phi}_{os}}{\hat{\Phi}_{oc}} \right), \quad (7)$$

where the caret (^) indicates an estimate.

The value of  $\hat{\theta}$  provides a single direction estimate between 0 and  $2\pi$  for each frequency bin using a four-quadrant arctangent calculation.

The output of the bearing calculation can be displayed similar to a LOFARGRAM. For a given PSD estimate, each frequency bin will have one bearing associated with it. With the frequency on the x-axis and the bearing on the y-axis, the plot indicates a bearing estimate for every frequency bin; this display format is referred to as a B-scan plot.

A user-selectable threshold can be applied to the B-scan display to show only bearings that have sufficient amplitude on the LOFARGRAM to be of interest. This threshold is generally set to remove all bearings from the B-scan display that are not of interest; this assumes that signals-of-interest are of significantly greater amplitude than undesirable narrowband or broadband acoustic noise.

### 3. FOS ALGORITHM

The fast orthogonal search (FOS) [7-15] is a general purpose modelling technique which can be applied to the estimation of difference equations, sums of exponential functions, and sinusoidal time-series models. The algorithm works by minimizing the mean-squared error (MSE) between a functional expansion of the time-series and the observed data.

An input function  $y(n)$  is fit to a functional expansion

$$y(n) = \sum_{m=0}^M a_m p_m(n) + \varepsilon(n) \quad (8)$$

where  $p_m(n)$  are arbitrary functions,  $a_m$  are the weights of the functional expansion, and  $\varepsilon(n)$  is the modelling error.

FOS begins by creating a functional expansion using orthogonal basis functions such that

$$y(n) = \sum_{m=0}^M g_m w_m(n) + e(n) \quad (9)$$

where  $w_m(n)$  is a selected orthogonal function,  $g_m$  is the weight of the function, and  $e(n)$  is an error term. The number of terms ( $M$ ) required to estimate the input signal with a chosen degree of error is defined as the model order.

The orthogonal functions  $w_m(n)$  are derived from the candidate functions  $p_m(n)$  using the Gram Schmidt (GS) orthogonalization algorithm. In this process, the GS

algorithm computes a set of weights  $\alpha_{mr}$ . The orthogonal functions are implicitly specified by the weights  $\alpha_{mr}$  and need not be computed explicitly.

In its last stage, FOS calculates the weights of the functional expansion,  $a_m$ , from the weights of the orthogonal series expansion,  $g_m$ , and the weights  $\alpha_{mr}$ , calculated by the GS algorithm.

A parsimonious model can be created by fitting terms which reduce the mean squared error (MSE) in order of their significance. The FOS search algorithm can be stopped:

- (a) when a certain number of terms is fitted;
- (b) when the ratio of MSE to the mean squared value of the input signal is below a threshold; or
- (c) when adding another term to the model reduces the MSE less than adding white Gaussian noise.

Spectral analysis with FOS is accomplished by selecting candidates  $p_m(n)$  that are pairs of sine and cosine terms at each of the frequencies of interest. Assuming a DC term is fitted as the first term, the candidate functions  $p_m(n)$  are given by

$$\begin{aligned} p_0(n) &= 1 \\ p_{2m} &= \cos(\omega_m n) \\ p_{2m+1} &= \sin(\omega_m n) \end{aligned} \quad (10)$$

where  $m=1, \dots, P$ ,  $\omega_m$  is the digital frequency of the candidate pair and  $P$  is the number of candidate pairs.

By fitting a sine and cosine pair at each candidate frequency, the magnitude and phase at the candidate frequency to be determined using the identities:

$$\begin{aligned} A \cos(\omega_m n) + B \sin(\omega_m n) &= C \cos(\omega_m n + \theta) \\ C &= \sqrt{A^2 + B^2} \\ \theta &= \tan^{-1}(B/A) \end{aligned} \quad (11)$$

FOS has been shown to be able to resolve two frequencies in the same FFT bin with up to 10 times the FFT resolution [10]. The improved resolution of FOS is achieved at the expense of computational complexity: the FFT computation is of order  $n \log n$ , FOS is of order  $Pn$ .

### 4. FOS BASED LOFARGRAM AND B-SCAN

The FOS algorithm can be used to estimate the PSD for the LOFARGRAM and B-scan algorithms. Unlike the FFT, FOS does not estimate the spectrum for every candidate frequency but fits a model with only significant, non-noise terms. The spectrum in the other frequency bins is assumed to be zero.

Although the omni, sine and cosine channels have the same frequency components, it has been observed that the FOS algorithm may select different candidate frequencies in the model for each channel due to the effects of noise. For the bearing estimate given in Eq. (7), the cross-spectral estimates of the omni-sine  $\hat{\Phi}_{os}$  and omni-cosine  $\hat{\Phi}_{oc}$  channels are required at exactly the same frequency. If the FOS models for the sine and cosine channels do not have calculated values at exactly the same frequencies, then the bearing estimates cannot be computed.

Since FOS creates a model based on the candidate functions made available to it, the algorithm can be forced to use certain candidates in the model, regardless of their MSE reduction.

From Eq. (1) it can be seen that the omni DIFAR channel will have the largest amplitude of the three channels. FOS will fit the strongest 25 frequency pairs in the omni-channel or it will stop when adding a new frequency pair fits less energy than adding a WGN term. These frequency pairs are then force-fit in the model for the spectral estimate of the sine and cosine channels. The result is a model that contains the same significant frequencies consistently across the three DIFAR spectral estimates allowing bearing estimates in these channels.

## 5. SIMULATION RESULTS

In the first simulation, two target signals that are too closely spaced to be discernible by DFT (but are discernible by FOS) are present. The second case involves using a frequency spacing for the two signals such that they are unresolvable by either FOS or DFT (i.e., they both lie in the same DFT and FOS bin). For B-scan, this implies that only one bearing can be found for the two sources.

Each target signal contains several narrowband frequency tones. Each signal consists of a time series created from a sum of sinusoids with noise added:

$$y(t) = \sum_{n=1}^{n_p} A_n \sin(2\pi F_n t + \varphi_n) + n(t), \quad (11)$$

where  $A_n$  and  $F_n$  and  $\varphi_n$  are the amplitude, frequency, and phase of the a single tone,  $n_p$  is the number of sinusoidal frequencies, and  $n(t)$  is omni-directional background noise. The phase added to each individual target signal was uniformly distributed between 0 and  $2\pi$ .

Two independent noise sources were added: the first to approximate propagation noise in the ocean, and the second to simulate receiver noise for each element of the array. Ambient noise is most certainly not white or Gaussian in nature [1], but it is a sufficient approximation for the purpose of this signal processing trial.

As seen in Eq. (1) the DIFAR signal is composed of 3

time series channels related to the omni channel such that

$$\begin{aligned} x_{\text{omni}}(t) &= \sum_{i=1}^T y_i(t) + n_o(t) + n_{o,r}(t) \\ x_{\text{sin}}(t) &= \sum_{i=1}^T y_i(t) \sin \theta_i + n_o(t) \sin \theta_i + n_{s,r}(t) \\ x_{\text{cos}}(t) &= \sum_{i=1}^T y_i(t) \cos \theta_i + n_o(t) \cos \theta_i + n_{c,r}(t) \end{aligned} \quad (12)$$

where  $y(t)$  is the synthetic signal at the source,  $x(t)$  is the signal at each channel,  $n_o$  is the ocean noise,  $n_{o,r}$ ,  $n_{s,r}$ , and  $n_{c,r}$  are the receiver noise for the omni, sine and cosine channels respectively. Here,  $\theta_i$  is the chosen direction-of-arrival angle of the synthetic target.

The signal-to-noise ratio (SNR) is defined as

$$SNR = 10 \log \left( \frac{\overline{x_{\text{omni}}(t)^2}}{\sigma_{\text{noise}}^2} \right) \quad (13)$$

where  $\sigma_{\text{noise}}^2$  is the variance of the noise and the overbar indicates the time-average. The variance of the noise approximating the ocean noise was adjusted to provide the amplitude of the noise  $n(t)$  to achieve the chosen SNR for each signal generated.

Two targets were introduced in the input signal whose powers are equal and bearing separation was varied from 180 degrees to 25 degrees at increments of 5 degrees. The detection was considered successful if the both estimated bearings were within 10 degrees of their respective input signal bearing. This was chosen since  $\pm 10$  degrees is the operationally accepted accuracy of a DIFAR sonobuoy [2]. In both simulations, 1000 realizations at each bearing were simulated in calculating the percent success.

For two targets with a bearing separation of 20 degrees or less, the bearings are spaced closer than the error tolerance of  $\pm 10$  degrees for each estimate. Hence 25 degrees was the minimum used in the simulations.

### 5.1. Two Sources - Separable

A time series was generated which contained two targets, one with a tonal at 54.9Hz and the other at 55.0Hz (i.e., a frequency separation of 0.1Hz). The bearing separation of the targets was varied from 180 to 25 degrees in 5 degree increments. The record length was 10 seconds (the entire time series required). Each 2-second time slice was extracted from the series as required, and the PSD for each channel was created from a five-slice average. The FFT and FOS resolutions (based on the input time series length) were 0.5Hz and 0.1 Hz respectively. FOS was stopped when 25 frequency pairs were fitted or when adding a term fitted no more energy than adding WGN



Sample plots of the bearing estimate with two sources separated by 90 degrees with an SNR of 3dB are in **Figure 1**. The figure shows the B-scan and LOFARGRAM displays for a representative spectral and bearing estimate. In the gram plots, a gray scale is used for the magnitude of FFT or FOS respectively. The gram plots are auto-scaled so that the largest magnitude in each gram is black and the lower magnitudes are shades or gray, while the lowest energy is white. In this case, the FFT bearing estimate shows two bearings, one of which appears correct. The bearing at 100 degrees (to the left of the input bearings) that appears correct is caused by spectral leakage, and as a result it is not in the bin where the signal is expected to be found. Since the energy in the Gram is low (below a threshold) this bearing estimate will be discarded as noise and typically

removed from the B-scan plot. By contrast, the FOS estimate (at right) has the input (diamond) and estimate (x) nearly co-located, indicating that both bearings are correct within  $\pm 10$  degrees of the true bearing.

**Figure 2** is a plot of the percent success for the B-scan technique for 1000 simulations at each bearing. Recall, an estimate is considered a "success" when the bearing estimate to both targets is within 10 degrees of the true bearing of the respective target. Note that the FFT B-scan method does not provide any successful estimates for SNR > 0 dB. By contrast, the FOS B-scan estimates vary from nearly 100 percent success and decrease with SNR. The plots are for four sample bearing separations of 75, 5, and 25 degrees, and nearly overlap. The variability of the curves and their overlap is due to noise

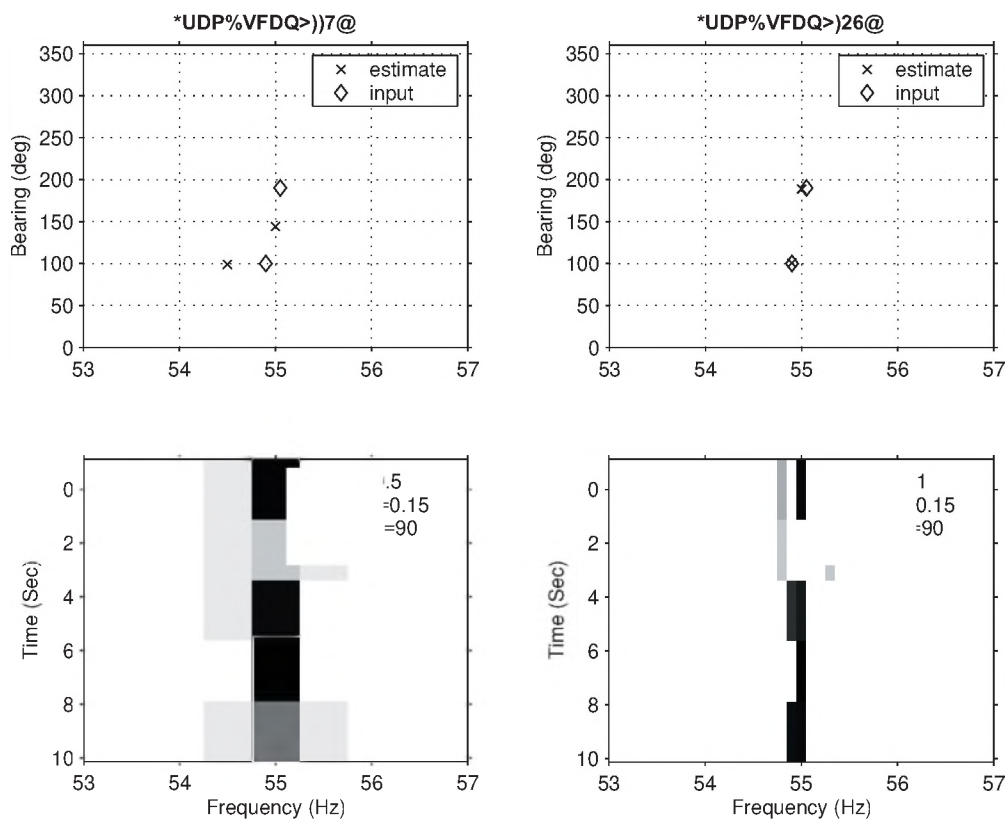


**Figure 1** The top left plot is the B-scan and bottom left plot is the Gram for the FFT method. The top right is the B-scan and bottom right is the Gram for the FOS method.

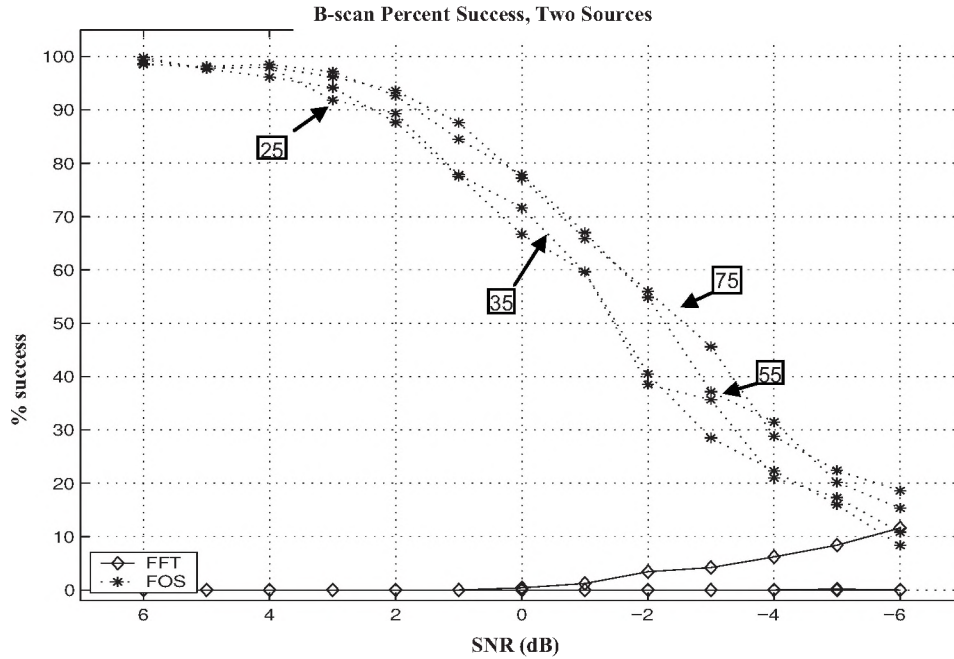


Figure 2: The four lines marked with the \*, from top to bottom, are the FOS B-scan percent success versus the SNR for two sources with a separation of 75, 55, 35 and 25 degrees, respectively. There are four lines for the FFT-Bscan as well, however, three of the lines are overlapping with a 0% success. The FFT-Bscan line that rises above the other three corresponds to a separation of 25 degrees.

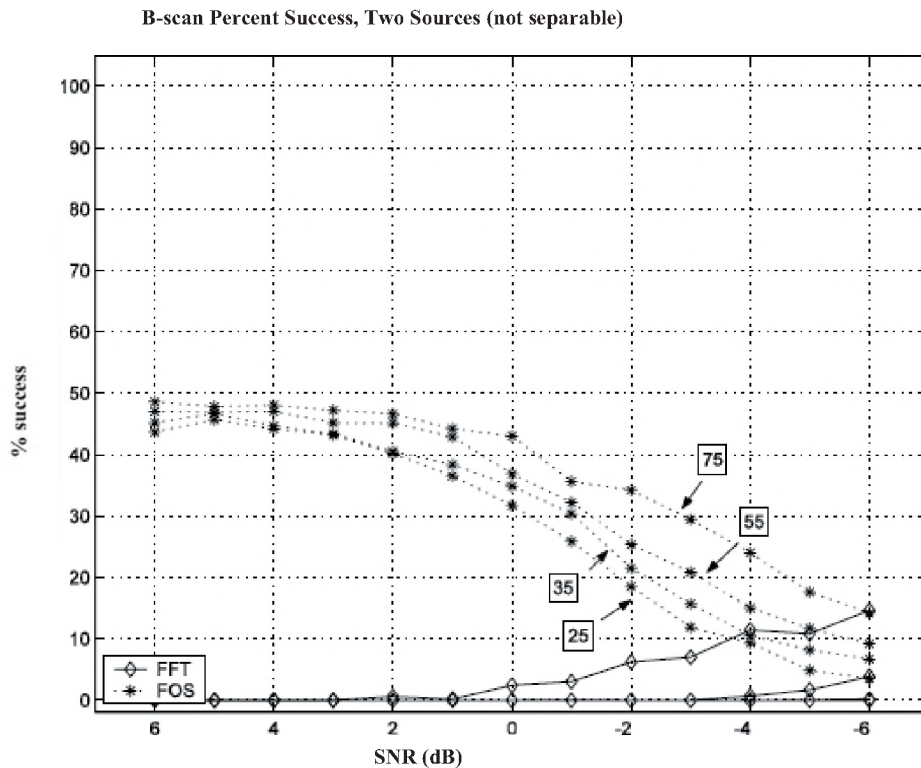


Figure 3: FFT and FOS B-scan percent success for two non-separable sources, versus SNR (dB). The four lines, from top to bottom, are angular separations of 75, 55, 35, and 25 degrees, respectively.

Note that for the FFT B-scan estimates, the percent success increases for two sources separated by 25 degree with an SNR of 0dB or less. These “successful” estimates are due to chance. They are caused by the noise biasing the B-scan estimates of two adjacent FFT bins to be within the  $\pm 10$  degree tolerance even though the signal is only present in one FFT bin.

## 5.2. Two Sources – Not Separable

In order to ensure consistency in the way FOS was employed, the frequency separation was decreased such that the two frequencies were in the same FOS bin. For this experiment the FOS resolution was 0.1Hz (as used in the previous experiment), while the target frequencies used were changed to 54.95Hz and 55.00Hz respectively (a separation of 0.05Hz).

As expected, neither B-scan was unable to resolve the two sources. The resulting bearing estimate for both FFT and FOS B-scan was generally a single estimate located between the two source bearings. The FFT B-scan percent success is zero at all SNR and all bearing separations. As shown in **Figure 3**, the FOS B-scan provided some successful estimates, but never more than one at a time (i.e., 50 percent success) given two input signals. Nonetheless, it clearly outperformed FFT B-scan again.

## 6. EXPERIMENTAL RESULTS

The comparison of Fourier and FOS-based bearing estimators was extended to more complex DIFAR data. Two data sets were used to compare the two techniques. The first data file was generated in the Operational Mission Simulator (OMS) at 14 Wing Greenwood Nova Scotia, while the latter data set was recorded by a real DIFAR sonobuoy deployed in the Atlantic Ocean.

### 6.1. Simulated DIFAR data

The OMS is a signal generator built by CAE electronics Inc. which creates complex acoustic signatures for multiple surface and submerged contacts as well as generating an ambient noise field to simulate ocean noise. It also generates RADAR, electronic sensing measures (ESM) signals, and is a full tactical crew trainer designed for ASW.

The data set contains three targets, two of which are merchant vessels, while the third is a submerged submarine. The submarine did not produce a continuous acoustic signature and was used only to create transient signals. The two merchant contacts are located north-east and south of the sonobuoy, and their acoustic signatures consist of multiple harmonics of frequencies in the 10-400 Hz spectrum.

**Figure 4** shows a plot of the relevant targets in the OMS scenario. Two merchant vessels and one submarine are present in the water. Sonobuoy positions are marked by  $\delta$  with the sonobuoy radio frequency (RF) number next to them. Sonobuoys are assumed to be stationary.

The presence of these three sound sources at the same time allowed an examination of specific frequency bins which were known to contain signals incident from more than one direction. A given FFT frequency bin could therefore be subdivided to a higher frequency resolution using FOS in order to separate the multiple sources and compare the directional estimates.

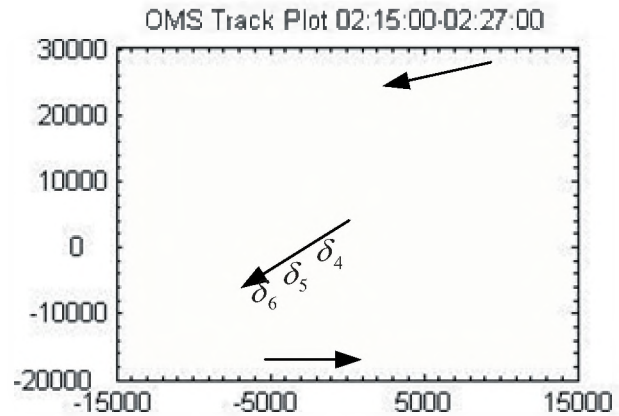


**Figure 4.** OMS track plot showing three targets and sonobuoys [4].

The PSD used for calculating bearing estimates was created from data that was averaged over 25 subsequent non-overlapped time slices of 5 seconds each. This results in an FFT resolution of 0.2Hz and 125 seconds of time-series data for each PSD point. The FOS resolution used in this section is 5 times the FFT resolution, or 0.04Hz. The FOS cross-spectral estimates are based upon the same length of time-series data.

From analysis not included in this paper, it was found that the signature of the vessel to the north-northeast (bearing of  $020^\circ$ ) contains both discrete sources and broadband noise. The vessel to the south-southwest had prominent lines (bearing of  $220^\circ$ ) at 27.4 and 42 Hz. There were clearly several instances where discrete frequency components of the two vessels overlap, (e.g. 42Hz).

**Figure 5** is a comparison of a FFT and FOS generated Gram/B-scan display between the frequencies of 22 and 27 Hz as in this frequency range two of the targets have signals in the same FFT bin. The time segment chosen is known to contain discrete lines from the merchant vessel to the north, but also contains broadband noise from the vessel to the south. The data analyzed is from the eastern most sonobuoy, labelled  $\delta_4$ .

The FFT gram (bottom-left) does not indicate any strong discrete spectral lines, and as such any bearings in the corresponding B-scan display would not necessarily be noted as significant by an operator. The FOS-generated gram (bottom-right) clearly shows two discrete sources present in the spectrum, and allows an assessment of their bearing in the corresponding B-scan display. Clearly identifiable in the FOS B-scan in **Figure 5** are two sources at B-scan bearings of  $020^\circ$  and  $270^\circ$  (the bearings are circled).

As FOS does not add model terms that are white Gaussian noise, the visible “salt-and-pepper” effect throughout the FOS gram indicates the presence of broadband coloured noise. This broadband noise is being fit into the FOS model.

The two targets in this scenario are at bearings of 20° and 220° respectively. Since B-scan bearings are biased by multiple sources present in a single frequency bin, the FOS B-scan bearing visible in the 22.6Hz at 270° is possibly a biased result due to the sources 220° and the broadband noise seen in the FOS B-scan.

Thus, the FOS B-scan was able to detect two bearings in the same FFT bin although the bearing for the target at 220° was biased due to the presence of broadband noise.

## 6.2. DIFAR Sonobuoy data

The data in this DIFAR recording are from a sonobuoy deployed from the CFAV QUEST during an acoustic trial.

The set contains three significant sources: two merchant vessels as well as an acoustic projector towed by the Quest. The sound sources are well distributed around the sonobuoy, with one vessel to the north heading easterly, one to the south heading westerly, and the QUEST towing an acoustic projector heading east-south-easterly. These data were used by Desrochers [3]. A surface plot of the geographical location of known targets for the data set is shown in **Figure 6**. The arrows indicate position and approximate motion of the vessels in the area. The sonobuoy positions are indicated by the  $\odot$  symbol. The data analyzed The DRDC data is from the eastern-most buoy just above the label 20:13 in **Figure 6**.

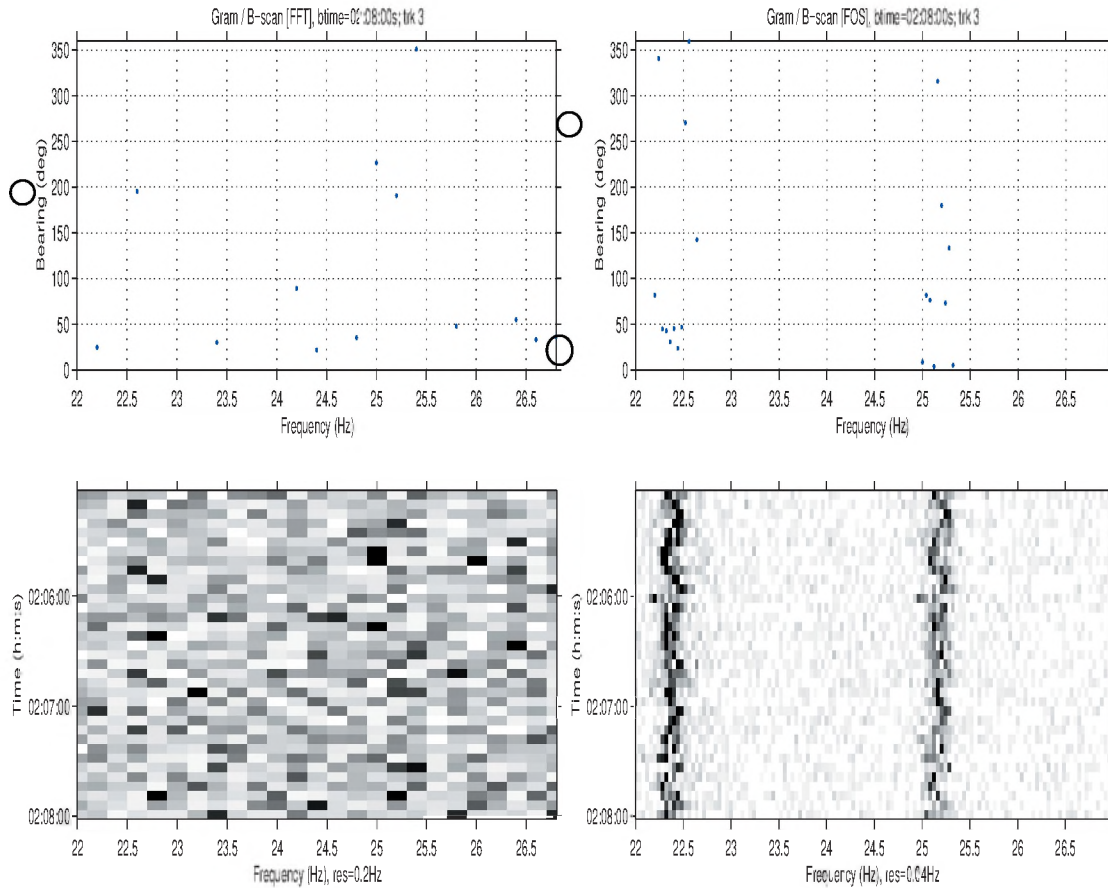


**Figure 5: The B-scan (top left) and Gram (bottom left) using the FFT, and the B-scan (top right) and Gram (bottom right) using FOS for OMS DIFAR data.**



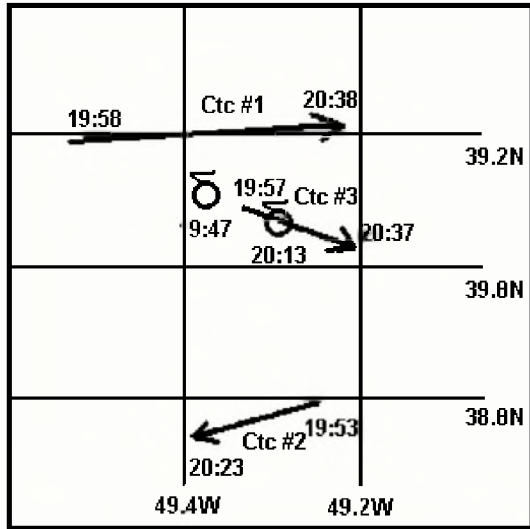


Figure 6: Surface plot of DRDC(A) DIFAR data. Extracted from Desrochers [3].

The DIFAR data set is 15 minutes long. The PSDs were estimated using a sample length of 5 seconds, resulting in a frequency resolution of 0.2 Hz. The data was averaged over 25 time slices for a total time of 125 seconds of time-series data for each row of the LOFARGRAM.

From analysis not included in this paper it was found that the towed projector generated discrete frequencies at 15, 17, 47, 49 and 147Hz at a bearing of approximately 130°. Broadband noise between 40 and 70Hz was found to be at a bearing of about 330°. Higher frequency broadband sources (above 80Hz) are found to the north-northwest, while an unknown source in the 30Hz range is at approximately 250°. A few bearings in the 80 to 110Hz range indicate the vessel known to be to the south of the sonobuoy.

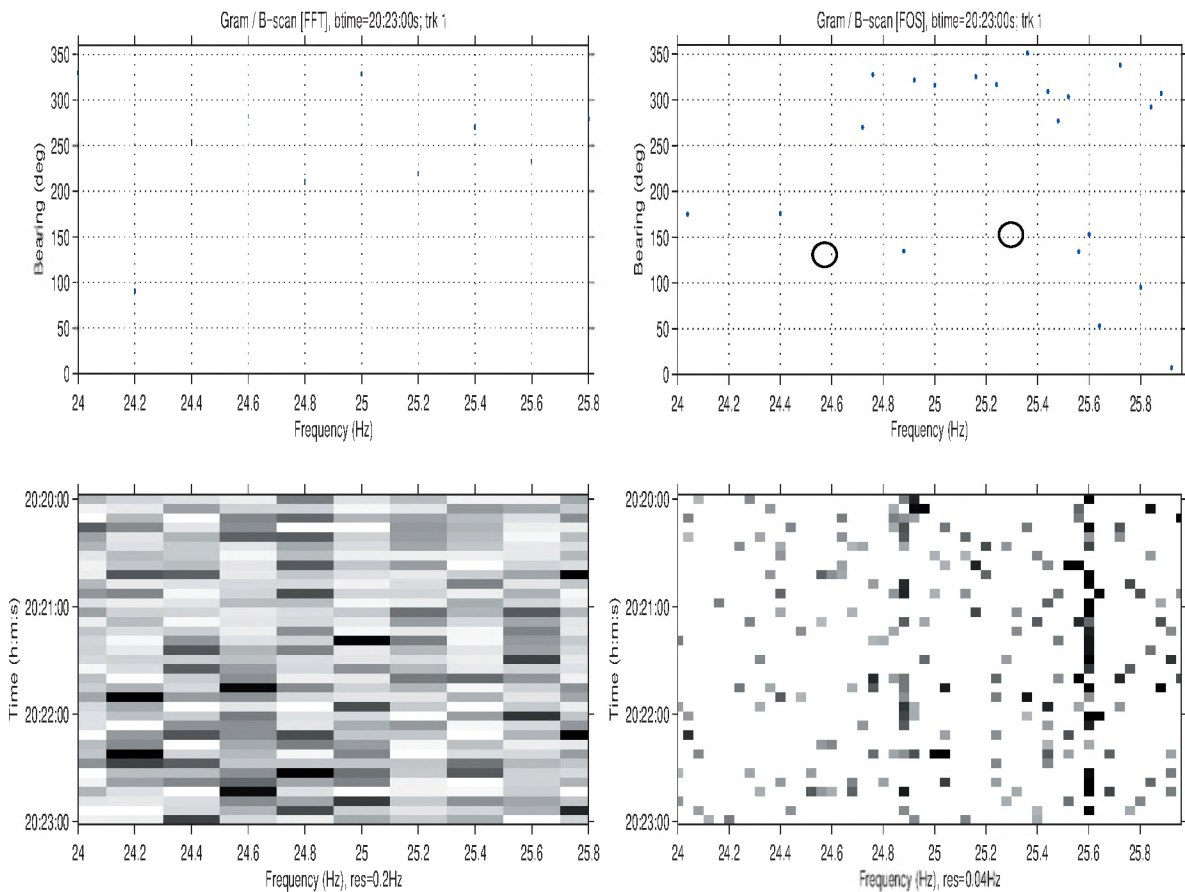


Figure 7: Comparison of FFT gram (top-left) and B-scan (bottom-left) and FOS gram (top-right) and B-scan (bottom-right) plots, for the DRDC(A) sonobuoy DIFAR data.

The frequency range between 22 and 26 Hz was examined where a known source existed but was not easily identifiable due to the presence of interference. The interference in this case was broadband noise from the merchant vessel to the north of the sonobuoy.

Twenty-five individual time slices of 5 seconds each were averaged to create the cross-spectral matrix (CSM) used for bearing calculations. The difference between the FFT-gram and FOS-gram and their corresponding B-scan estimates is seen in **Figure 7**. The FFT-gram does not show any discrete sources, while the corresponding B-scan plot shows diffuse bearings between 200° and 300°. By contrast, the FOS-gram shows the presence of two narrowband sources and identifies the corresponding bearings as 130° and 150° (circled on figure). These bearings indicate the source could be the QUEST, to the south-east of the sonobuoy. The broadband bearings are more clearly identified as being from a bearing of approximately 320°, and therefore from the merchant vessel to the north.

## 7. CONCLUSIONS

The FOS spectral estimation algorithm was used to perform a high resolution spectral estimate for use in the LOFARGRAM and B-scan algorithms. It was demonstrated that the FOS based algorithms could distinguish between two sources whose frequencies were in the same FFT bin, if the sources were separable by FOS. The probability of success was 0.7 or higher when the signals' SNR was 0 dB or greater. FOS B-scan was able to estimate two bearings, whereas the FFT B-scan could only estimate one bearing. Additionally, FOS provided one accurate estimate for a pair of signals in one FOS bin, where an FFT estimate yielded no accurate estimates. The improved resolution of the FOS based algorithms was demonstrated in simulation and on experimental DIFAR data.

## 8. ACKNOWLEDGEMENT

The author's thank 14 Wing Greenwood Nova Scotia for the OMS simulated data. The DIFAR sonobuoy data was provided by Dr. Ian Fraser at DRDC(A) and all the data was demodulated by DRDC(A). The work was supported by an NSERC Discovery Grant and the Academic Research Program at RMC.

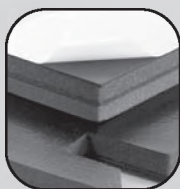
## 9. REFERENCES

- [1] R. J. Urick, *Principles of underwater sound*, Revised ed. New York: McGraw-Hill, 1975.
- [2] B. H. Maranda, "The Performance of the Arctangent Bearing Estimator in Isotropic Noise," *DREA Technical Memorandum TM 1999-145*, 1999.
- [3] D. Desrochers, "High resolution Beamforming Techniques Applied to a DIFAR Sonobuoy," in *Physics Department*. Kingston: Royal Military College of Canada, 1999.
- [4] D. M. Weston, "DIFAR bearing estimation using wavelet transforms," in *Physics Department*. Kingston: Royal Military College of Canada, 2002.
- [5] E. C. Ifeachor and B. W. Jervis, *Digital signal processing a practical approach*, 2nd ed. Harlow, England: Prentice Hall, 2002.
- [6] J. G. Proakis and D. G. Manolakis, *Digital signal processing principles, algorithms, and applications*, 3rd ed. Upper Saddle River, N.J: Prentice Hall, 1996.
- [7] M. J. Korenberg, "Fast orthogonal identification of nonlinear difference equations and functional expansion models," vol. 1 pp. 270-276, 1987.
- [8] M. J. Korenberg, "A robust orthogonal algorithm for system identification and time-series analysis," *Biological Cybernetics*, vol. 60 pp. 267-276, 1989.
- [9] M. J. Korenberg and K. M. Adeney, "Iterative Fast Orthogonal Search for Modeling by a Sum of Exponentials or Sinusoids," *Annals of Biomedical Engineering*, vol. 26, pp. 315-327, 1998.
- [10] D. McGaughey, M. J. Korenberg, K. M. Adeney, and S. D. Collins, "Using the Fast Orthogonal Search with First Term Reselection to Find Subharmonic Terms in Spectral Analysis," *Annals of Biomedical Engineering*, vol. 31 pp. 741-751, 2003.
- [11] D. McGaughey, "Spectral Modelling and Simulation of Atmospherically Distorted Wavefront Data," in *Electrical Engineering*. Kingston: Queen's University, 2000.
- [12] K. H. Chon, M. J. Korenberg, and N. H. Holstein-Rathlou, "Application of Fast Orthogonal Search to Linear and Nonlinear Stochastic Systems," *Annals of Biomedical Engineering*, vol. 25, pp. 793-801, 1997.
- [13] K. H. Chon, "Accurate Identification of Periodic Oscillations Buried in White or Colored Noise Using Fast Orthogonal Search," *IEEE Transactions on Biomedical Engineering*, vol. 48, pp. 622-629, 2001.
- [14] K. Nutt, "Speed-Sensorless Control of Three-Phase Induction Motors: A study into the Application of Fast Orthogonal Search Algorithm to Speed-Sensorless Control of AC motors," in *Electrical Engineering*. Kingston: Royal Military College, 2001.
- [15] Y. T. Wu, M. Sun, D. Krieger, and R. J. Scلابassi, "Comparison of Orthogonal Search and Canonical Variate Analysis for the Identification of Neurobiological Systems," *Annals of Biomedical Engineering*, vol. 27, pp. 592-606, 1999.

# Better testing... better products.

## The Blachford Acoustics Laboratory

Bringing you superior acoustical products from the most advanced testing facilities available.



Our newest resource offers an unprecedented means of better understanding acoustical make-up and the impact of noise sources. The result? Better differentiation and value-added products for our customers.

### Blachford Acoustics Laboratory features

- Hemi-anechoic room and dynamometer for testing heavy trucks and large vehicles or machines.
- Reverberation room for the testing of acoustical materials and components in one place.
- Jury room for sound quality development.



### Blachford acoustical products

- Design and production of simple and complex laminates in various shapes, thicknesses and weights.
- Provide customers with everything from custom-engineered rolls and diecuts to molded and cast-in-place materials.

**Blachford** **QS 9000**  
REGISTERED

[www.blachford.com](http://www.blachford.com) | Ontario 905.823.3200 | Illinois 630.231.8300

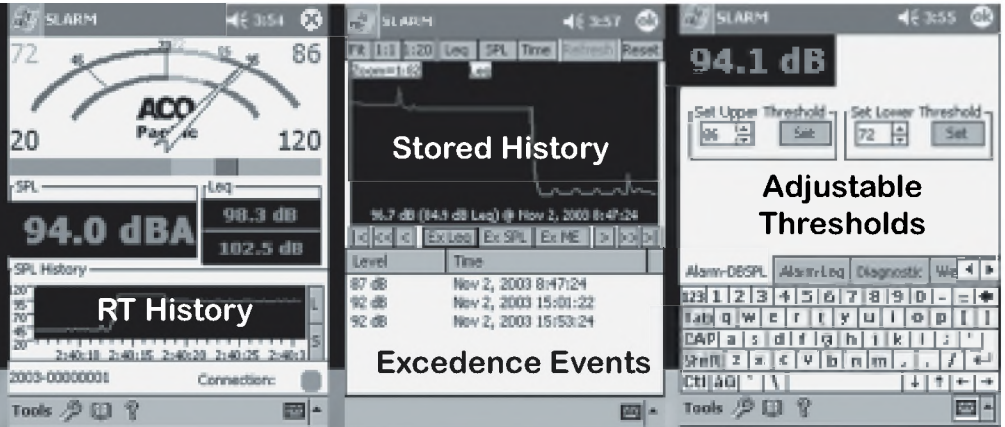




# Noise Pollution

## The SLARM™ Solution

PDA & Laptop  
Displays  
Wired  
Wireless



The SLARM™ developed in response to increased emphasis on hearing conservation and comfort in the community and workplace incorporates ACOustAlert™ and ACOustAlarm™ technology. Making the SLARM™ a powerful and versatile sound monitoring/alarm system.

### Typical Applications Include:

#### Community

- ◆ Amphitheatres
- ◆ Outdoor Events
- ◆ Nightclubs/Discos
- ◆ Churches
- ◆ Classrooms

#### Industrial

- ◆ Machine/Plant Noise
- ◆ Fault Detection
- ◆ Marshalling Yards
- ◆ Construction Sites
- ◆ Product Testing

### FEATURES

- √ Wired and Wireless (opt)
- √ USB, Serial, and LAN(opt) Connectivity
- √ Remote Displays and Programming
- √ SPL, Leq, Thresholds, Alert and Alarm Filters (A,C,Z), Thresholds, Calibration
- √ Multiple Profiles (opt)
- √ 100 dB Display Range:
- √ 20-120 dBSPL and 40-140 dBSPL
- √ Real-time Clock/Calendar
- √ Internal Storage: 10+days @1/sec
- √ Remote Storage of 1/8 second events
- √ 7052S Type 1.5™ Titanium Measurement Mic

2604 Read Ave., Belmont, CA 94002 Tel: 650-595-8588 FAX: 650-591-2891  
www.acopacific.com acopac@acopacific.com

## ACOustics Begins With ACO™

